Heat-capacity studies near the smectic-A—smectic-C (—smectic-C^*) transition in a racemic (chiral) smectic liquid crystal

S. C. Lien and C. C. Huang

School of Physics and Astronomy, Univeristy of Minnesota, Minneapolis, Minnesota 55455

J. W. Goodby

AT&T Bell Laboratories, Murray Hill, New Jersey 07974

High-resolution heat-capacity measurements have been carried out on the chiral and racemic versions of 2-methylbutyl-4'-n-pentyloxy-biphenyl-4-carboxylate (2M45OBC). Both smectic-A—smectic-C and smectic-A—chiral-smectic-C transitions are found to be mean-field-like with a large sixth-order term in the Landau free-energy expansion. Our results also shed light on similarities and differences between the chiral and racemic compounds.

I. INTRODUCTION

A variety of organic compounds exhibit the smectic-A (SmA) and, at lower temperature, the smectic-C (SmC) liquid-crystal phase characterized by a one-dimensional density wave which has a wave vector along (A), or tilted with respect to (C) the average long molecular axis (director). If the constituent molecules are optically active, the chiral smectic-C (SmC^*) phase will be observed instead of the SmC phase. In the SmC^* phase, as a consequence of the molecular chirality, the director exhibits a helical structure precessing around the direction perpendicular to the smectic layers. In 1973, de Gennes[1] proposed that the SmA-SmC transition might be continuous and might exhibit heliumlike critical behavior (three-dimensional XY model). In early heat-capacity measurements by Shantz and Johnson on one liquid-crystal compound [4-n-pentylphenylthio-4'-n-octyloxybenzoate ($\overline{8}$S5)],[2] raw data showed mean-field behavior in the vicinity of the SmA-SmC transition. Applying Landau-Ginzburg criterion to their x-ray data on $\overline{8}$S5, Safinya et al.[3] argued that the heat-capacity jump at the transition temperature and bare correlation lengths characterizing tilt-angle fluctuations are so large that the critical region is very small and beyond experimental resolution. Furthermore, Huang and Viner[4] have pointed out the importance of retaining the sixth-order term in the Landau free-energy expansion in order to provide quantitative explanation of heat-capacity data obtained near one SmA-SmC transition. Afterward the significance of the sixth-order term has been further confirmed in all the materials being studied near the SmA-SmC transition.[5-7]

In 1975 Meyer et al.[8] established the existence and the behavior of ferroelectric liquid crystals which showed the SmC^* phase and observed a rather small difference in the SmA-SmC transition temperatures between the chiral and racemic versions of p-decyloxybenzylidene-p-amino-2-methylbutylcinnamate (DOBAMBC). This and other experimental evidence indicate that the SmA-SmC^* transition is mainly driven by intermolecular forces producing the SmC phase and not by ferroelectric coupling between permanent dipoles.[9] The spontaneous polarization is thus a secondary rather than a primary order parameter.[10] In other words, the energy associated with the interaction between permanent dipoles is only a small perturbation of the system. Thus a similar transition between SmA-SmC and SmA-SmC^* transitions would be expected. To quantitatively address this question we will report *first* high-resolution heat-capacity measurement on the racemic and chiral versions of one liquid-crystal compound, i.e., 2-methylbutyl-4'-n-pentyloxy-biphenyl-4-carboxylate (2M45OBC). Our results not only show that both SmA-SmC (racemic version) and SmA-SmC^* (chiral version) transitions are well described by the mean-field Landau model including sixth-order terms but also shed light on similarities and differences between these two versions.

II. RESULT

A high-resolution calorimetric investigation of both the racemic and chiral configurations of 2M45OBC has been carried out in the vicinity of SmA-SmC and SmA-SmC^* transitions, respectively. The detail of our measurement technique has been reported elsewhere.[11] The liquid crystals were contained in a chemically etched sample cell with dimensions 1.02-cm diameter by 0.15-mm deep. The top and bottom cover glasses which formed the sample cell were chemically etched down to 25 μm in thickness in order to reduce the addendum heat-capacity contribution. The total heat capacity per unit area C_A^{tot} (liquid crystal and addenda) was calculated from $(I^2 R/A)/(\sqrt{2}\omega\Delta T)$. Here an ac heating current I (rms value), operated at the angular frequency ω, was passed through a gold resistance film with resistance R and area A. ΔT is the measured rms temperature-oscillation amplitude. In order to figure out the addendum contributed (glass slides, thermocouples, G.E. varnish, etc.) to C_A^{tot}, we measured the heat capacity of a glass slide, with 50 μm thick, of the same material as that of the sample cells. It was found that addenda contributed 25% and 28% to C_A^{tot} for chiral and racemic samples, respectively. After subtracting the addendum heat capacity per unit area (C_A^{add}), the liquid-
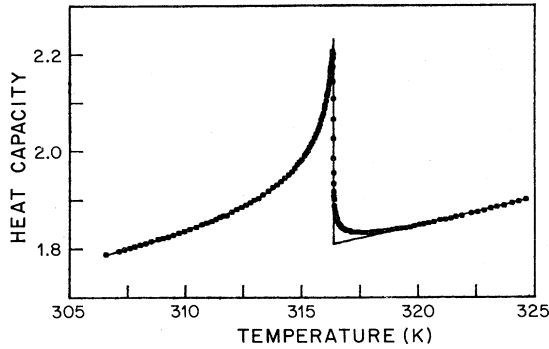
FIG. 1. Heat capacity in J/cm^3 K vs temperature in degrees K near the SmA-SmC* transition of chiral 2M45OBC. Squares, experimental data; solid line, best fit to Eqs. (2) and (3).

TABLE I. Transition temperature and important parameters near the SmA-SmC and SmA-SmC* transition of 2M45OBC. T_1 is the isotropic-SmA transition temperature and T_c is the SmA-SmC or SmA-SmC* transition temperature.

Compound	T_1	T_c	$10^3 \times t_0$	$\Delta C_J{}^a$
Racemic	63.81	42.854	3.9	0.35
Chiral	63.81	43.200	3.5	0.41

^{a}Heat-capacity jump at T_c in the unit of J/cm^3 K.

crystal heat capacity per unit volume was calculated by $C = (C_A^{tot} - C_A^{add})/d$, where d is the thickness of the sample. The d's were measured by employing an optical microscope and a mechanical gauge. The thicknesses d determined by these methods were further checked by the measured high cutoff frequency (ω_H).[12] ω_H was determined from the 3 dB point in the frequency response curve at a given fixed temperature and

$$\frac{1}{\omega_H^2} = \frac{(2\pi)^2}{90} \left[[(2d_g)C_g + dC] \left[\frac{2d_g}{K_g} + \frac{d}{K} \right] \right]^2 ,$$

where C_g, K_g, and d_g are the heat capacity per unit volume, thermal conductivity, and thickness of glass, respectively. K is the thermal conductivity of the liquid-crystal sample. The factor of 2 in the terms involving glass comes from the fact that the sample was sandwiched between two pieces of glass. Now $C_g \simeq C$, $K \simeq 0.1 K_g$ (Ref. 13), and $d/d_g = 6$. Therefore, to a good approximation ω_H is inversely proportional to $(2d_g + d)d$.

The measured heat capacity per unit volume (C) for the chiral and racemic version of 2M45OBC is shown in Figs. 1 and 2, respectively. The fact that both heat-capacity curves are nearly linear functions of temperature over a 1 and 2, respectively. The fact that both heat-capacity curves are nearly linear functions of temperature over a
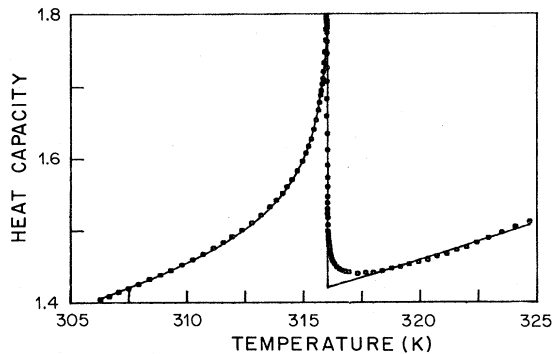
wide temperature range (319–325 K) above the transition and have abrupt jumps indicates that the nature of these two phase transitions is dominantly mean-field-like. No anomalous phase shifts ($\lesssim 8 \times 10^{-3}$ rad) between the input heater voltage and the sample temperature response were observed during the course of our experimental runs. Between successive heating and cooling runs of heat capacity versus T no thermal hysteresis was observable within the relative temperature resolution of the experiment (± 3 mK). Consequently, we conclude that both SmA-SmC and SmA-SmC* transitions are continuous.

The measured transition temperatures are shown in Table I. Both isotropic—SmA and SmC (SmC*)—crystalline phase transitions show hysteresis and have large phase shifts (> 0.25 rad). Consequently, they are first-order phase transitions.

III. DATA ANALYSIS AND DISCUSSION

In the course of investigating the nature of SmA-SmC transitions, Huang and Viner[4] suggested that retaining the sixth-order term in the Landau free-energy expansion is crucial to explain their measured heat-capacity data as well as resolve the discrepancy among the reported critical exponents associated with the tilt angle. The heat-capacity anomalies shown in Figs. 1 and 2 are characterized by the same features as the ones for the other SmA-SmC transitions. Namely, the heat capacity is approximately a linear function of temperature in the SmA phase and there exists an abrupt jump of the heat capacity with the 10—90% width being equal to 3×10^{-4} in reduced temperature. Consequently, we will use the heat-capacity expression obtained from the following free energy to fit our data

$$G = G_0 + at\Psi^2 + b\Psi^4 + c\Psi^6 , \qquad (1)$$

where Ψ is the order parameter (i.e., tilt angle), $t = (T - T_c)/T_c$, and T_c is the transition temperature. G_0 is the nonsingular part of free energy and $(a,b,c) > 0$ for a continuous transition. From Eq. (1) one obtains[4]

$$C = \begin{cases} C_0 & \text{for } T > T_c \\ C_0 + AT(T_m - T)^{-1/2} & \text{for } T < T_c \end{cases} \qquad (2)$$

where $T_m = T_c(1 + t_0/3)$, $t_0 = b^2/ac$, and $A = a^{3/2}/[2(3c)^{1/2}T_c^{3/2}]$. C_0 is the background heat capacity obtained from G_0. Here we assumed that

$$C_0 = B + Dt + Et^2 \qquad (3)$$

both above and below T_c. Here T_c is chosen to be the

FIG. 2. Heat capacity in J/cm^3 K vs temperature in degrees K near the SmA-SmC transition of racemic 2M45OBC. Squares, experimental data; solid line, best fit to Eqs. (2) and (3).

TABLE II. Parameters obtained from fittings with quadratic background for the chiral 2M4SOBC. A in $J/cm^3 K^{3/2}$ and B, D, and E in $J/cm^3 K$.

Case	Fitting range	T_M (K)	$A \times 10^4$	B	D	E	χ_v^2
I	$-3.1 \times 10^{-2} < t < -3.1 \times 10^{-4}$	316.694	7.72	1.808	3.32	6.93	1.33
	$9.0 \times 10^{-3} < t < 2.8 \times 10^{-2}$	±0.010	±0.07	±0.003			
II	$-3.1 \times 10^{-2} < t < -7.9 \times 10^{-4}$	316.715	7.80	1.808	3.34	7.20	1.18
	$9.0 \times 10^{-3} < t < 2.8 \times 10^{-2}$	±0.009	±0.06	±0.003			
III	$-3.1 \times 10^{-2} < t < -2.4 \times 10^{-3}$	316.689	7.74	1.808	3.33	7.22	1.23
	$9.0 \times 10^{-3} < t < 2.8 \times 10^{-2}$	±0.010	±0.07	±0.003			
IV	$-3.1 \times 10^{-2} < t < -7.9 \times 10^{-4}$	316.556	7.48	1.81	3.25	2.33	3.65
	$4.6 \times 10^{-3} < t < 2.8 \times 10^{-2}$	±0.020	±0.10	±0.04	±0.04	±0.02	

midpoint of the heat-capacity jump in the temperature axis. The data were fitted to Eqs. (2) and (3) with one set of fitting parameters, i.e., T_m, A, B, D, and E. The fitting results for the chiral compound are shown in Table II. The solid curve in Fig. 1 corresponds to case II in Table II. Under similar circumstances, one obtains the solid curve in Fig. 2 for the racemic version.

The fact that the ratio of the last two terms in Eq. (3), i.e., Et^2/Dt, is less than 9% for the racemic compound and 5% for the chiral one within entire fitting ranges indicates that results with quadratic background term should be close to that with linear one. Indeed, the parameters T_m, A, B, and D obtained in the fitting scheme with the linear background term, i.e., fitted to Eqs. (2) and (3) with $E = 0$, differ from those obtained with quadratic background term by less than 2.2% for the chiral version and 5.5% for the racemic modification. Though the two fitting schemes give similar results, corresponding χ squares show that the fitting with quadratic background is definitely better, especially for the racemic compound. Two important parameters (i.e., t_0 and the size of the heat-capacity jump at T_c) obtained through the fitting to Eqs. (2) and (3) are shown in Table I for the racemic and chiral compounds, respectively.

Experimentally the isotropic-SmA transition temperatures are the same for the chiral and racemic versions. This is consistent with the picture that in both isotropic and SmA phases the molecules can freely rotate around their long axes. Consequently, the lack of macroscopic polarization leads to the same isotropic-SmA transition temperatures. On the other hand, SmA-SmC^* transition temperature is higher than the corresponding SmA-SmC one by 0.35 K. Based on a simple theory, Meyer[9] has argued that the SmA-SmC^* transition temperature will be enhanced with respect to the corresponding SmA-SmC transition through the coupling between the tilt angle and the macroscopic polarization. The existence of macroscopic polarization in the SmC^* phase means that rotation along the molecular long axis is partially frozen. However, the synthesis process of the chiral compounds is dif-

ferent from that of the racemic one. Each of these compounds showed a single spot in the thin-layer chromatographic analysis. The elemental analysis showed that the ratios of the constituent elements are within ±0.1% of the calculated values. Still these two high-quality compounds may have a trace of different impurities. Even if the impurities are the same, the shifts of transition temperatures caused by impurities may be different for different kinds of phase transitions. Studies on other high-quality samples may shed further light on our observed difference in the transition temperatures.

The uncertainty ($\sim 10\%$) in determining the heat capacity per unit volume of the sample mainly comes from the measurement of sample thickness d. Incidentally, this seems sufficient to explain that the heat capacity per unit volume of the chiral version is larger than that of the racemic version by about 20%. However, the fact that $\omega_H(\text{chiral})/\omega_H(\text{racemic}) = 1.18 \pm 0.06$ and $[(2d_g + d)d]$ $(\text{racemic})/[(2d_g + d)d](\text{chiral}) = 1.16$ are equal leads us to rule out that this difference is entirely due to thickness uncertainties. The heat capacity measures the energy-energy correlation. Our result indicates that energy-energy correlation of chiral molecules with the same chirality is higher than the case with different chirality even in the SmA
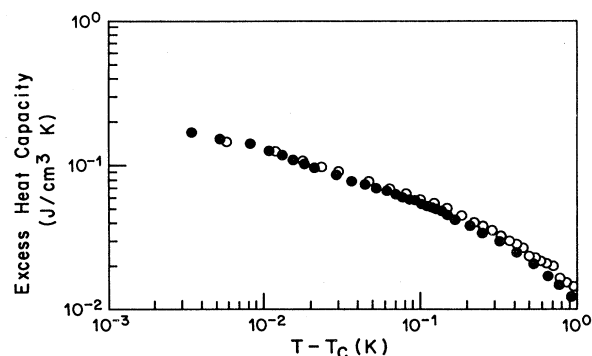

FIG. 3. Excess heat capacity vs $T - T_c$ for chiral (open circles) and racemic (solid dots) compounds.

phase.

After subtracting the fitted curve from the measured data, excess heat capacity is obtained for $T > T_c$. The results are shown in Fig. 3. There are no differences in the excess heat capacity between the chiral and racemic compounds within our experimental resolution. This suggests that the fluctuation heat capacity due to polarization or pitch fluctuations just above the $\text{Sm}A\text{-Sm}C^*$ transition is much smaller than that due to tilt-angle fluctuations. Finally, Lien et al.[14] have observed excess heat capacity in addition to the mean-field heat capacity for both $T > T_c$ and $T < T_c$ in the vicinity of $\text{Sm}A\text{-Sm}C^*$ transition of DOBAMBC. We do not have an explanation why there exists excess heat capacity for $T < T_c$ in DOBAMBC of the chiral version but not in 2M45OBC.

ACKNOWLEDGMENTS

[1]P. G. de Gennes, Mol. Cryst. Liq. Cryst. 21, 49 (1973).
[2]C. A. Shantz and D. L. Johnson, Phys. Rev. A 17, 1504 (1978).
[3]C. R. Safinya, M. Kaplan, J. Als-Nielsen, R. J. Birgeneau, D. Davidov, J. D. Litster, D. L. Johnson, and M. Neubert, Phys. Rev. B 21, 4149 (1980).
[4]C. C. Huang and J. M. Viner, Phys. Rev. A 25, 3385 (1982).
[5]C. C. Huang and S. C. Lien, Phys. Rev. Lett. 47, 1917 (1981).
[6]R. J. Birgeneau, C. W. Garland, A. R. Kortan, J. D. Litster, M. Meichle, B. M. Ocko, C. Rosenblatt, L. J. Yu, and J. Goodby, Phys. Rev. A 27, 1251 (1983).
[7]M. Meichle and C. W. Garland, Phys. Rev. A 27, 2624 (1983).
[8]R. B. Meyer, L. Liebert, L. Strzelecki, and P. Keller, J. Phys. Lett. (Paris) 36, 69 (1975).
[9]R. B. Meyer, Mol. Cryst. Liq. Cryst. 40, 33 (1977).
[10]J. W. Goodby, G. W. Gray, and D. G. McDonnell, Mol. Cryst. Liq. Cryst. Lett. 34, 183 (1977).
[11]J. M. Viner, D. Lamey, C. C. Huang, R. Pindak, and J. W. Goodby, Phys. Rev. A 28, 2433 (1983).
[12]P. Sullivan and G. Seidel, Phys. Rev. 173, 679 (1968).
[13]P. Pieranski, F. Brochard, and E. Guyon, J. Phys. (Paris) 33, 681 (1972).
[14]S. C. Lien, J. M. Viner, and C. C. Huang (unpublished).